

4

2003 02 05 224

DTIC FILE COPY

AD-A213 803

THE EFFECT OF DISSOLVED CHLORINE ON THE
PITTING BEHAVIOR OF 304L STAINLESS STEEL
IN A 0.5 N NaCl SOLUTION

H.H. Lu and D.J. Duquette
Rensselaer Polytechnic Institute
Materials Engineering Department

OCTOBER 1989

Technical Report to the Office of Naval Research
Contract No. N00014-89-J-1125

Reproduction in whole or in part for any purpose of the U.S.
Government is permitted. Distribution of this document is
unlimited.

DTIC
ELECTE
OCT 30 1989
S E D

89 10 27 092

The Effect of Dissolved Chlorine on the
Pitting Behavior of 304L Stainless Steel
in a 0.5 N NaCl Solution



H.H. Lu and D.J. Duquette
Department of Materials Engineering
Rensselaer Polytechnic Institute
Troy, New York 12180-3590

Accession For	
NTIS GRA&I	<input checked="" type="checkbox"/>
DTIC TAB	<input type="checkbox"/>
Unannounced	<input type="checkbox"/>
Justification	
By _____	
Distribution/	
Availability Codes	
Dist	Avail and/or Special
A-1	

The Effect of Dissolved Chlorine on the
Pitting Behavior of 304L Stainless Steel
in a 0.5 N NaCl Solution

H.H. Lu and D.J. Duquette
Department of Materials Engineering
Rensselaer Polytechnic Institute
Troy, New York 12180-3590

Abstract

Electrochemical experiments were performed on a 304L stainless steel alloy in a 0.5 N NaCl solution as a function of chlorine content (0-180 mg/l). Experiments performed included a measurement of the corrosion potential as a function of time, the determination of the breakdown potential, and of the repassivation potential, utilizing cyclic polarization curves; and the use of a scratching electrode technique to measure the kinetic aspects of the breakdown of passivity. The addition of chlorine to a solution of pH 5 in the concentration range of 20-60 ppm chlorine resulted in a significant shift in the corrosion potential in the noble direction. At higher concentrations of chlorine the corrosion potential shifts back toward that observed without chlorine additions. Chlorine also results in a monotonic shift in the breakdown potential, suggesting that the passive film is rendered more stable against the initiation of localized corrosion. However, the repassivation potential exhibits a minimum in the chlorine concentration range where the corrosion

potential exhibits a maximum. This data suggests that the rate of propagation of localized corrosion should be maximized in this chlorine regime (20-60 mg/l). When scratching electrode experiments are performed, the number of pits is minimized but the size of the pits is maximized. Analysis of the kinetic pit growth results suggest that, when the pits are small, the rate of pit growth is controlled by diffusion of corrosion products through the bulk aqueous phase, but, as the pits age, the mechanism changes, and pit growth is governed by diffusion through a solid or semi-solid film on the walls of the pits.

Keywords: Diffusion, Liquid Phases, Solid Films, (AW)

**The Effects of Dissolved Chlorine on the
Pitting Behavior of 304L Stainless Steel
in a 0.5N NaCl Solution**

H.H. Lu and D.J. Duquette
Department of Materials Engineering
Rensselaer Polytechnic Institute
Troy, New York 12180-3590

Introduction

Chlorine added to water is a potent algaecide and bactericide, and has been used in a number of applications to reduce biofouling and/or biocorrosion. However, the noble redox potential for the Cl_2/Cl^- reaction suggests that passive metals or alloys in chlorine containing solutions may be susceptible to pitting and/or crevice corrosion if chlorine is dissolved in solutions which contain chlorides. However, a literature survey conducted by NACE in 1976 resulted in the discovery of only 30 publications related to chlorinated water, (most related to wet chlorine) and only 19 publications related to chlorinated brines. (1) None of these studies were directly related to stainless steels.

More recently, Goodman, in a review of the effects of chlorination on materials for sea water cooling systems concluded that there are few data available related to the effects of chlorine on the corrosion behavior of ferrous alloys in general and still less on the behavior of stainless

alloys.⁽²⁾ Some recent studies, primarily performed in chlorinated sea water, have been performed on a number of stainless alloys (3-6), with mixed results. For example, it has been shown that, for low levels of chlorine (<0.1ppm) the drift of corrosion potential in the noble direction which is generally observed in sea water for 300 type steels was inhibited. However, a large, stable shift in the corrosion potential was measured, and both pitting and crevice corrosion were observed on the free surfaces of the alloy, although crevice corrosion in an artificial crevice was no worse than for unchlorinated waters. The accelerated corrosion phenomenon due to chlorine was shown to be highly temperature dependent, with corrosion of even highly resistant alloys being observed at 40°C, but little corrosion being observed at 15°C.^(4,6) Pitting and crevice corrosion also have been observed in 22Cr-8Ni-3Mo with chlorine levels of 1 mg/l.⁽³⁾ The noble shift in the corrosion potential has been attributed to an alternative cathodic reaction due to the reduction of dissolved oxygen:⁽⁴⁾

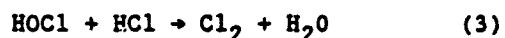


If the shift in the corrosion potential due to surface reaction is sufficiently electropositive, the pitting potential may be exceeded, and either pitting or crevice corrosion can be expected. This investigation examines the pitting tendency of an 18Cr - 8Ni stainless steel in chlorinated sodium chloride solutions.

Experimental Procedure

Potentiodynamic anodic polarization experiments, as well as scratching

electrode experiments, were performed on a vacuum melted 304L stainless steel in solutions containing 0.5N sodium chloride at room temperature (25±3°C). The alloy composition is shown in Table I. Chlorine concentrations were controlled between 0 and 180 mg/l by the addition of sodium hypochlorite (NaOCl), and the pH of the solution was controlled with the addition of HCl. Chlorine is generated in this system accordingly to the reactions:



The bulk of the experiments conducted were at a pH of 5.0. At this pH the primary species present is HOCl (Figure 1). Specific chlorine concentrations were measured for each experiment utilizing the standard DPD method (7). In addition to experiments conducted at pH5, pH for some experiments was varied between pH1 and pH5. An additional variable included a preliminary study of the effects of cathodic reduction of the alloy surface prior to polarization in order to examine the role of the stability of the air formed film against localized corrosion.

The specimen geometry was approximately 1 cm x 1 cm x 0.3 cm. Polarization samples were mounted in epoxy. Specimen surfaces were wet ground to 600 grit on SiC paper. For most experiments the specimen was held at -1.0 V vs. SCE for five minutes, and a one hour exposure at the rest potential followed by an anodic polarization scan. Polarization scan rates were performed at 10 mV/sec and the breakdown potential, E_b , and the repassivation potential, E_p , were determined from the polarization

scans, performed first in the noble direction followed by a reverse scan, in the active direction.

A limited study of the kinetics of pit growth was performed by fixing the potential at a value noble to the pit nucleation potential, scratching the specimen surface, and monitoring the resultant increase in current density. These experiments were performed at room temperature, in a 0.5 N NaCl solution of pH5, with 0, 20, and 60 mg/l chlorine.

Results and Discussion

Figure 2 shows anodic and cathodic polarization curves for 304L stainless steel, cathodically reduced at -1.0 V vs. SCE for 5 minutes, in 0.5 N NaCl solutions containing 20 mg/l and 60 mg/l chlorine, at room temperature. Similar data were generated for a chlorine concentration of 180 mg/l but are not shown for clarity. In each solution the alloy shows a marked hysteresis behavior, indicating that crevice corrosion can be expected, and be a significant problem in the presence of chlorine. Additionally, increasing the chlorine concentration of the solution shifted the corrosion potential in the noble direction by approximately 300-400 mv.

A similar shift in the zero current potential, as derived from the polarization curves also is observed, although the maximum potential in this case occurs at 60 rather than 20 mg/l dissolved chlorine (figure 3). The scatter in this data, as determined from triplicate tests, is the order of ± 30 mv. The difference in these values are believed to be due to the relatively short time for the polarization experiment compared to the measurements of the free corrosion potential. For low concentrations of chlorine the steady state conditions on the alloy surface are sluggish

compared to the situation for more concentrated chlorine solutions. Accordingly, the corrosion potential tends to appear to be somewhat more noble than the zero-current potential for chlorine concentrations less than 60 mg/l. At higher chlorine concentrations the values are similar.

The breakdown potential and the repassivation potential as a function of dissolved chlorine concentration are shown in figure 4. The breakdown potential increases monotonically with increasing chlorine concentrations, from a value of $-+ 0.050$ mv vs. SCE at 0 mg/l chlorine to a value of $-+ 0.400$ mv vs. SCE at 180 mg/l dissolved chlorine. The repassivation potential, on the other hand, exhibits a minimum at approximately 20 mg/l and increases for larger concentrations of chlorine. If the data of figures 3 and 4 are plotted on the same diagram, figure 5, it can be seen that in the chlorine concentration range of 10-60 mg/l, the corrosion potential is in fact noble to the repassivation potential. In this chlorine concentration regime then, localized corrosion initiated in crevices can be expected to freely propagate, although, as the chlorine concentration is increased, the resistance to the initiation of localized corrosion is increased. The scatter in these data, as determined from triplicate tests is also of the order of ± 30 mv.

Thus, it is apparent from these data that the effect of dissolved chlorine on the localized corrosion behavior of 18-8 stainless steels is more likely to be manifested in a propensity for crevice corrosion in this chlorine concentration range of 10-60 mg/l. Accordingly, a series of experiments was conducted wherein the passive film was mechanically ruptured by scratching and the resultant current density was measured as a function of time after scratching. The results of these experiments are shown in Figures 6-9. For example, figure 6 shows the increase in current

density for a specimen held at 50, 100 and 200 mv vs. SCE, respectively in 0.5 NaCl solution without chlorine additions ($E_b = 0.046$ v, $E_p = 0.122$ v vs. SCE). The data shown here are as expected, and indicate a large increase in current density shortly after scratching, followed by a region of steady state corrosion. These data are suggestive of rapid initiation followed by transport limited pit growth.

Figures 7, 8, and 9 show these data for 20 and 60 mg/l dissolved chlorine and exhibit similar trends. At 20 mg/l chlorine however, ($E_b = 0.195$ v and $E_p = -0.238$ v vs. SCE) the initial data at +100 mv vs. SCE are unstable, suggesting an attempt to repassivate the alloy surface. (figure 7a) At intermediate applied potentials (200 mv and 250 mv vs. SCE) steady state pit growth is observed immediately after initiation; while at the highest applied potential, a slight increase in current (or pit growth) with time is observed. At 60 mg/l dissolved chlorine ($E_b = 0.263$ mv vs. $E_p = -200$ mv vs. SCE) a small perturbation in current occurs for an applied potential of +100 mv vs. SCE. At higher applied potentials there is a large initial increase in current density followed by a steady state, virtually constant, current suggesting steady state pit growth.

It has been suggested that the time dependence of pit initiation and growth on passive metals and alloys obeys a relationship: (8)

$$i_t = i_p + A(t - t_I)^m \quad (4)$$

where

- i_t = total measured current density
- i_p = passive current density
- t_I = incubation time
- A, m = constants which are a function of transport conditions and pit geometry.

For the experiments described here the passive current density i_a can be assumed to approach zero and since the surface is scratched to initiate localized corrosion, $t_I \rightarrow 0$. Therefore this equation simplifies to:

$$i = A t^m \quad (5)$$

or

$$\log i = \log A + m \log t \quad (6)$$

The data of figures 6a - 8a can thus be described on a log-log plot, and if the equation is valid, the constants A and m can be determined from the plot. Figures 6b - 8b show this data, and indicate that each of sets of data for figures 6a - 8a can be reduced to either one or two slopes; the first slope related to a transient condition (pit initiation) and the second to pit propagation.

For most of the initial or transient pit growth (with the exception of a solution containing 60 mg/l chlorine at 100 mv vs. SCE), the slopes lie between 0.5 and 1.0, with a mean value of 0.6 - 0.7. (Table II)

This value can be rationalized by considering the geometry of the pits (assumed to be circular on initiation and to grow hemispherically) and the assumptions that the growth of the pits is controlled by transport processes.

The relationship between the linear growth of a hemispherical pit, and time can be expressed as (8):

$$r = c^3 \sqrt{A} t^2 \quad (7)$$

and, for transport control

$$r = \frac{C^3 \sqrt{i}}{Z} \quad (8)$$

where

$$C = \frac{3}{\sqrt{3V_m}} \frac{1}{8\pi F} \quad (9)$$

In these equations, r is the pit radius, V_m is the specific volume of the metal, F is Faraday's constant, and Z is the number of pits.

It can be shown from simple measurements and calculations that for each of these cases considered here $Z \cdot r^2$ is equal to a constant (Table III) and thus the current density should scale as r^2/C^3 , and the slope of $\log i$ vs. time should have a slope of $2/3$. It is assumed that the deviation of some of the measured slopes from $2/3$ is a result of the absence of purely hemispherical pits (a geometric factor) and the assumption that all pits are of the same size. In any case it can be concluded that initial pit growth is essentially the same for both unchlorinated and chlorinated sodium chloride solutions, is diffusion controlled through the liquid phase, and initially is not influenced by the age of the pits. Figure 9a and 9b show a slope of 0.67 superimposed on the transient current data from figures 6b and (unchlorinated, +200 mv vs. SCE) and 7b (20 mg/l chlorine, + 200 mv vs. SCE) and show the excellent fit of the data for potentials noble to the breakdown potential.

However, the second slope obtained for each set of experiments, which generally approaches zero (Table II), indicated that the pits approach a steady state growth rate, where transport control through a solid or semi-solid film governs the process. Further evidence of this type of behavior as the pits age is the faceted appearance of the pits

as shown in Figure 10. This faceted appearance is indicative of slow transport through a solid or semi solid film.

Pit Distribution and Morphologies

Although the kinetic values of pit growth are virtually independent of the chlorine concentration of the solution, the interaction between pit initiation and growth are quite different, depending on the chlorine concentration. Table III shows the average pit density for samples measured at the conclusion of the polarization experiments, as well as the mean pit size and the maximum pit size measured in a 1 cm² area. These data indicate that the number of pits per unit area is large with no dissolved chlorine, but that the mean pit size is small and correlates well with the maximum pit diameter. At 20 mg/l dissolved chlorine (the most active repassivation potential and the most noble corrosion potential) the pit density is at a minimum, while the pit diameter is a maximum. As the amount of chlorine in solution is increased, the pit density increases and, in general the pit size decreases. Thus, the pit size, and the pit density correlate with the differences between the repassivation potential and the corrosion potential. At values of 20 to 60 mg/l dissolved chlorine, the number of pits is relatively low and the pit size is relatively large. This suggests that, at these concentrations pit growth occurs readily, while initiation of new pits is more difficult. At lower and higher concentration of chlorine, large numbers of pits are observed, initiation is easy but growth of the pits is inhibited. Thus, the morphological characteristics of the pits correlate well with the differences between the breakdown and repassivation potentials. These differences, exhibiting a maximum between 20-60 mg/l

chlorine, suggest that crevice corrosion (essentially a pit growth process) can be expected to be a factor in this concentration range. The distribution and morphology of pits in a solution containing 20 mg/l chlorine is shown in Figure 11.

To summarize, it appears that chlorine, a strong oxidant, stabilizes the passive film against pit initiation as measured by the breakdown potential. However, at intermediate concentrations, when breakdown occurs, pit growth is enhanced. At very high concentrations the strong oxidizing potential of the chlorine apparently inhibits pit growth, probably due to a repassivation process. Since the inside of a pit can be expected to be acidified, a series of experiments was conducted as a function of pH on the corrosion potential, the breakdown potential, and the repassivation potential at a chlorine concentration of 20 mg/l. The results of these experiments are shown in Table IV. These data indicate that, as the pH is reduced, the difference between the breakdown potential, and the repassivation potential approach zero, indicating that the resistance to pit growth is reduced. Since at these low pH's Cl_2 dominates the dissociation of the hypochlorite, it is likely that the Cl_2 is directly reduced to Cl^- , thus, effectively increasing the chloride concentration in the pits and accordingly inhibiting repassivation.

Conclusions

1. The addition of chlorine to a 0.5 M NaCl of pH5 resulted in a marked shift in the corrosion potential of the alloy in the noble direction. This shift is a maximum of -300 mv at a chlorine

concentration of 20 mg/l, and decreases with further chlorine addition to only -50 mv at 180 mg/l. A similar shift is observed in the zero current potential of a potentiodynamic polarization curve, but the maximum is observed at -60 mg/l chlorine.

2. The addition of chlorine to a chloride solution also results in a shift of both the breakdown potential and the repassivation potential in the noble direction. While the shift in the noble direction of the breakdown potential indicates an increased resistance to the initiation of localized corrosion, there is a cross-over between the corrosion potential and the repassivation potential in the range 10-60 mg/l chlorine. This behavior suggests that the propagation of localized corrosion can be expected to be accelerated. Measurements of pit density and size confirm this conclusion in that, in the range of 20-60 mg/l dissolved chlorine, the pit density is markedly decreased, but the pit size is sharply increased.

3. The results of the pit growth experiments can be interpreted by the development of a more stable passive film created by the strong oxidation potential of the chlorine. Thus, while pit initiation is inhibited as indicated by the more noble breakdown potential, there can be expected to be a stronger driving force for pit growth due to the larger potential difference between the more stable passive film and the interior of an active pit.

4. The mechanism of pit growth and early propagation appears to be similar, and is believed to be controlled by diffusion of soluble species from the interior of the pit through the liquid phase in the pits. However, as the pits become larger, pit propagation rates are reduced. The rate controlling step for larger pits is believed to be due to diffusion through the solid or semi-solid film on the surface of the pits.

Acknowledgments

The authors gratefully acknowledge the support of the Office of Naval Research and, in particular, Dr. A.J. Sedricks under contract number N00014-86-K-0194.

References

1. NACE TPC Publication No. 4 "A Bibliography of Corrosion by Chlorine" NACE, Houston, 1976.
2. P.D. Goodman, Br. Corros. J., 22, 56 (1987).
3. E.B. Shone and P. Gallagher, Proc., Conf. on High Alloy Steels for Critical Sea Water Applications, Birmingham, Mar. 1985, Society of Chemical Industry, Materials Preservation Group.
4. R.E. Malpas, P. Gallagher and E.B. Shone, Proc. Conf. on Chlorination of Sea Water and Its Effect on Corrosion Behavior, Birmingham, Mar. 1986, Society of Chemical Industry, Materials Preservation Group.
5. R. Francis, in Stainless Steels '87, Institute of Metals, London, 1988, p. 182.
6. R.E. Malpas, P. Gallagher and E.B. Shone, in Stainless Steels '87, Institute of Metals, London, 1988, p. 253.
7. Standard Methods for the Examination of Water and Waste Water, 15th ed., Ed. M.A.H. Franson, Am Health Assoc. Washington, P. 227.
8. J. Tousek, in Theoretical Aspects of the Localized Corrosion of Metals, Trans. Tech. Publications, 1985.
9. J.W. Oldfield and B. Todd, Desalination, 1981, 38, 233.

**Table 1. Chemical Composition of 304L Stainless Steel
Used in This Study.**

C	Mn	P	S	Si	Cr	Ni	Mo	Cu	N	Co
0.016	1.55	0.009	0.016	0.70	18.82	9.72	0.05	0.10	0.04	0.10

**Table 2. Exponential Values of Pit Growth Constants, m ,
in Equation $i = A t^m$**

Chlorine Concentration (mg/L)

Applied mV vs SCE	0		20		60	
	m_1	m_2	m_1	m_2	m_1	m_2
50	0.6	--	--	--	--	--
100	0.9	0.22	--	0.5	0.5	--
150	1.0	0.29	--	--	--	--
200	--	--	0.6	0.005	0.33	--
250	--	--	0.5	0.009	0.46	0.24
300	--	--	0.5	--	--	--

Table 3. Pit Characteristics.

C(Cl ₂) (mg/L)	Pit density (1/cm ²)	Mean pit size (mm)	Cross section area of average pit (mm ²)	Max. pit size (mm)	Pit density x average pit area
0	1495	0.047	1.73×10^{-3}	0.07	2.6×10^{-2}
20	280	0.126	1.24×10^{-2}	0.30	3.5×10^{-2}
60	724	0.260	5.3×10^{-2}	0.40	3.8×10^{-2}
180	2522	0.033	8.5×10^{-4}	0.09	2.1×10^{-2}

Table 4. Effect of PH on the Corrosion Potential, the Breakdown Potential and the Repassivation Potential in 0.5N NaCl Solution Containing 20 mg/L Chlorine.

PH	E _{corr} (V)	E _b (V)	E _p (V)	E _b - E _p (V)
1.03	-0.433	-0.118	-0.118	0
2.05	-0.467	0.010	-0.100	0.110
3.00	-0.259	0.190	-0.163	0.353
4.01	-0.274	0.280	-0.160	0.440

List of Figures

Figure 1. Variation of chlorine distribution in sea water as a function of PH ⁽⁹⁾

Figure 2. Typical cyclic polarization curves for 304L stainless steel in chlorinated, 0.5N NaCl solution at 0, 20, and 60 mg/L dissolved chlorine.

Figure 3. Steady state corrosion potentials (open circuit) and zero current potentials as a function of dissolved chlorine concentration for 304L stainless steel in 0.5N NaCl solution.

Figure 4. Breakdown and repassivation potentials as a function of chlorine concentration for 304L stainless steel in 0.5N NaCl solution.

Figure 5. A comparison of corrosion potential, zero current potential, breakdown potential and repassivation potential for stainless steel in 0.5N NaCl solution as a function of dissolved chlorine concentration.

Figure 6. Current density vs time after scratching at constant potentials for 304L stainless steel in 0.5N NaCl solution (0 mg/L dissolved chlorine).

Figure 7. Current density vs time after scratching at constant potentials for 304L stainless steel in 0.5N NaCl solution with 20 mg/L dissolved chlorine.

Figure 8. Current density vs time after scratching at constant potentials for 304L stainless steel in 0.5N NaCl solution with 60 mg/L dissolved chlorine.

Figure 9 Correlation between measured slope of current density vs time with a hypothetical slope of 0.67 for transient period of localized corrosion of 304L stainless steel in 0.5N NaCl solution (a) Unchlorinated (b) 20 mg/L dissolved chlorine.

Figure 10. Typical morphology of pits in 304L stainless steel in 0.5N NaCl solution. Pit morphology is unchanged by chlorination (a) Optical cross-section (b, c) Scanning electron micrographs

Figure 11. Pit distribution on 304L stainless steel in 0.5N NaCl solution with 20 mg/L dissolved chlorine.

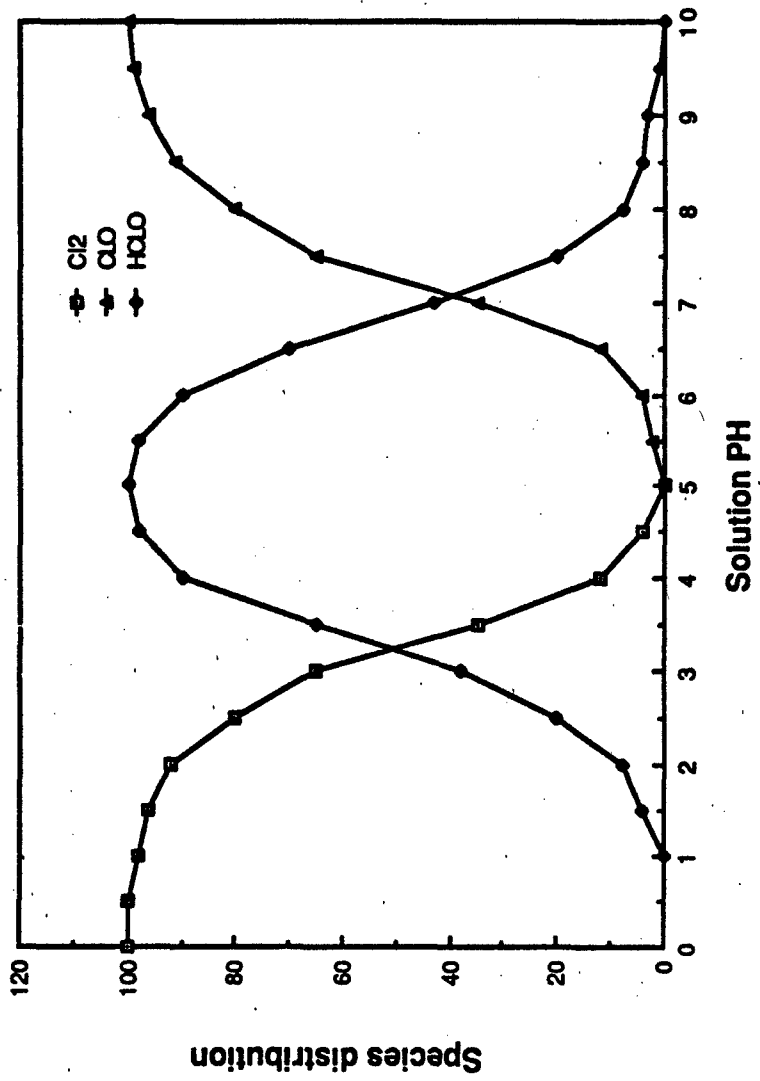


Fig.1 The relative concentration of chlorine in the PH range (9)

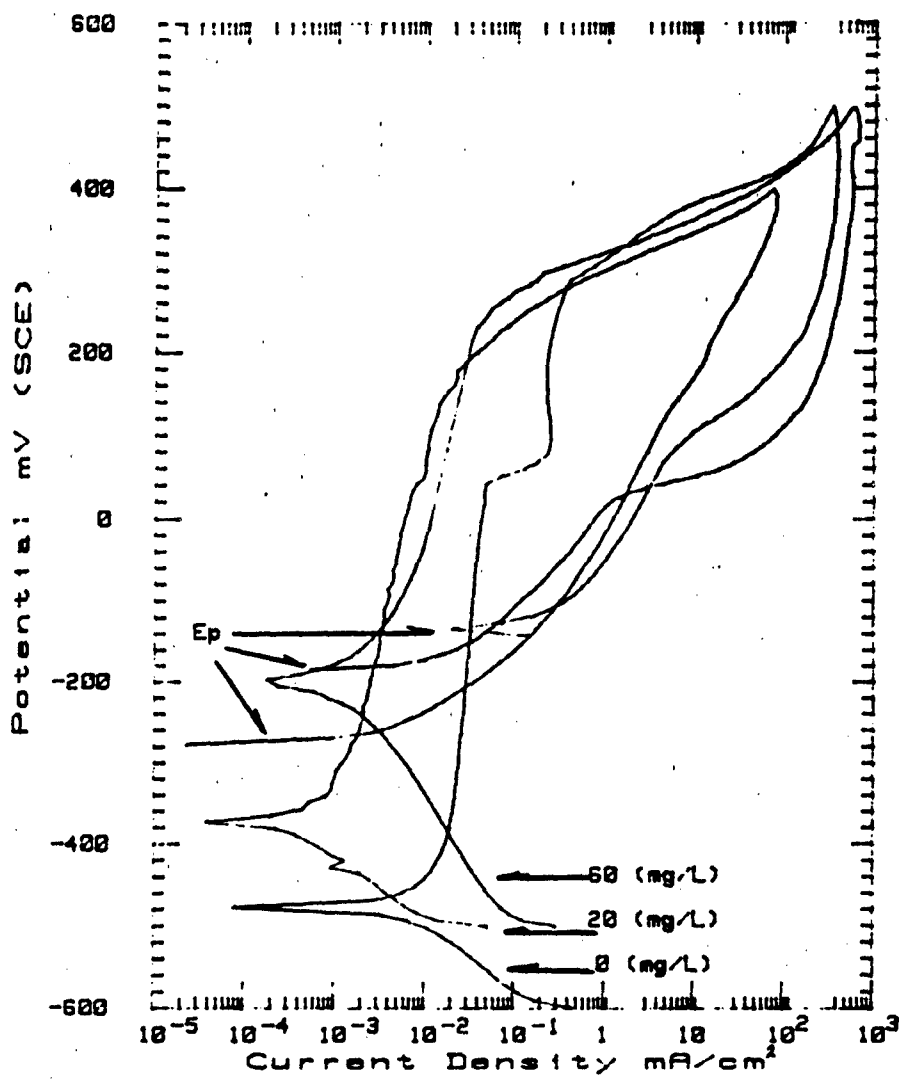


Figure 2. Typical cyclic polarization curves for 304L stainless steel in chlorinated, 0.5N NaCl solution at 0, 20, and 60 mg/L dissolved chlorine.

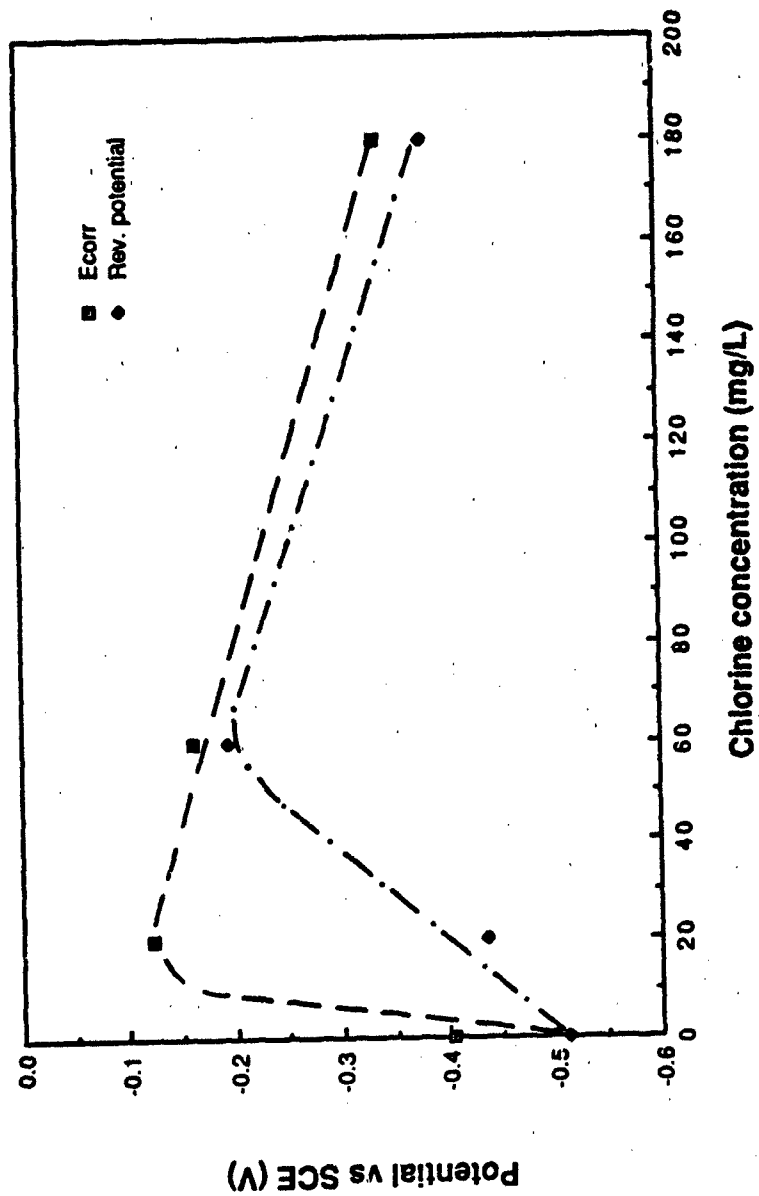


Figure 3. Steady state corrosion potentials (open circuit) and zero current potentials as a function of dissolved chlorine concentration for 304L stainless steel in 0.5N NaCl solution.

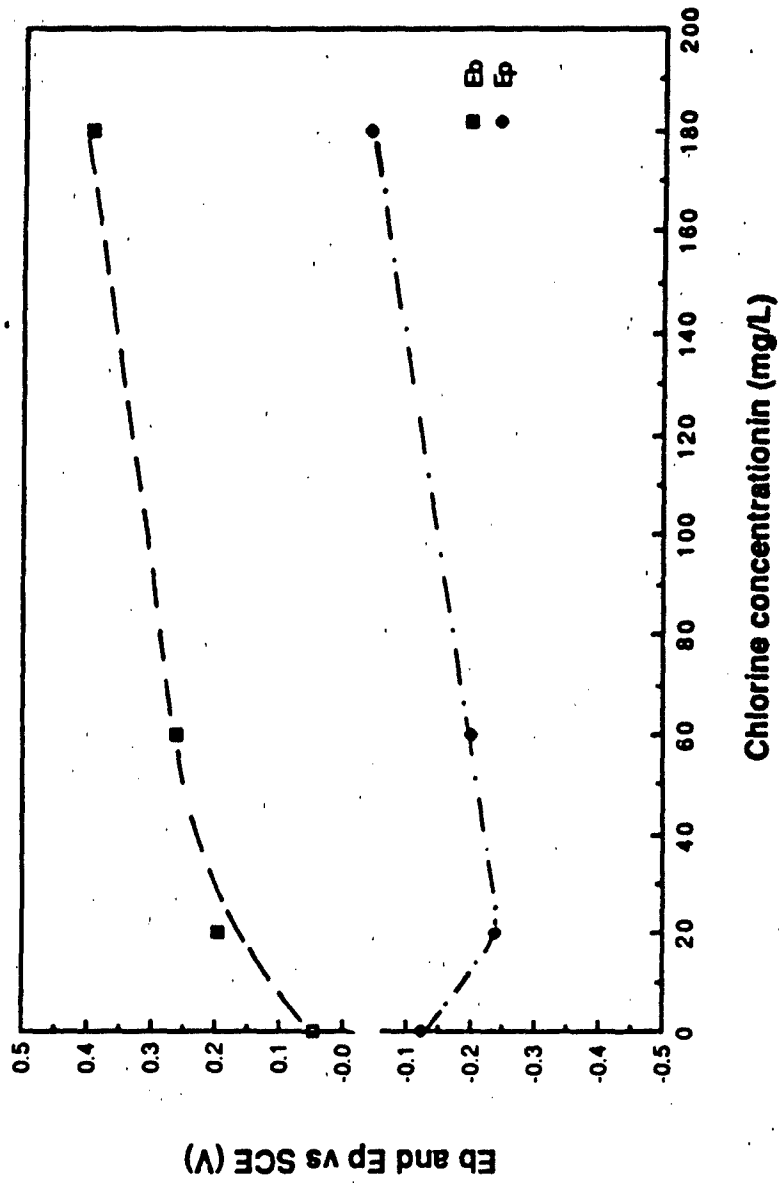


Figure 4. Breakdown and repassivation potentials as a function of chlorine concentration for 304L stainless steel in 0.5N NaCl solution.

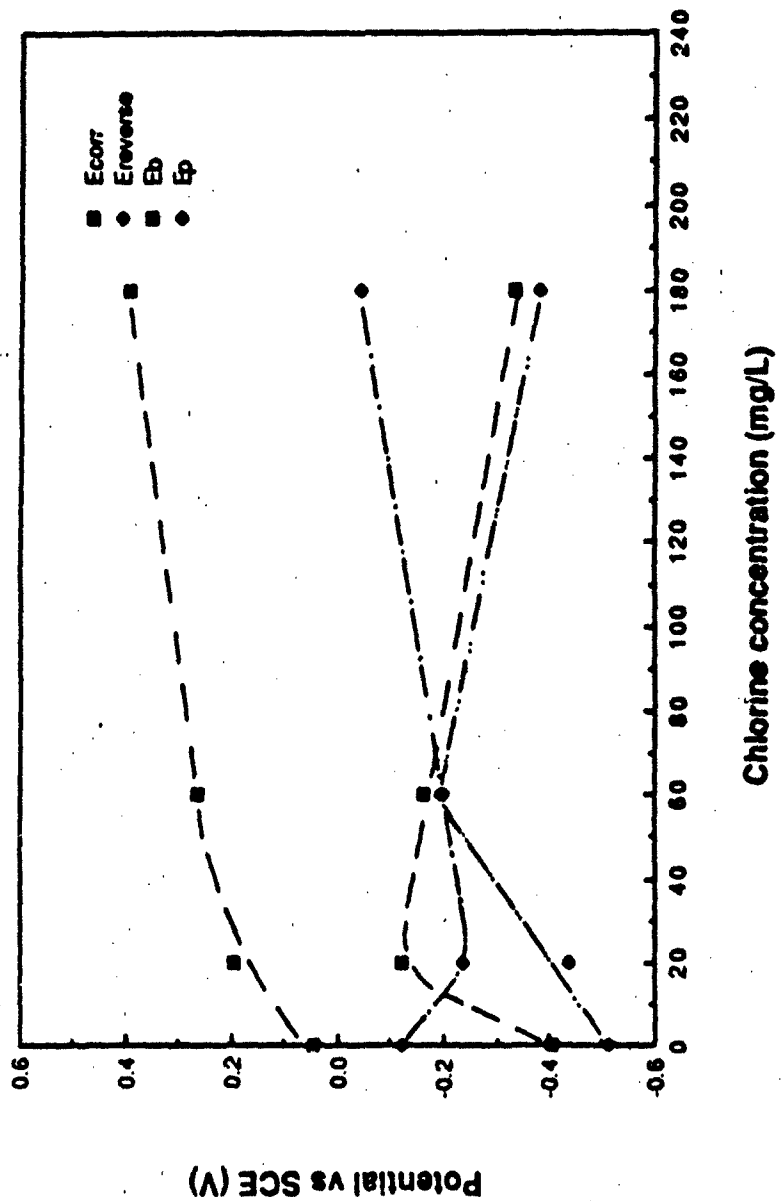


Figure 5. A comparison of corrosion potential, zero current potential, breakdown potential and repassivation potential for stainless steel in 0.5N NaCl solution as a function of dissolved chlorine concentration.

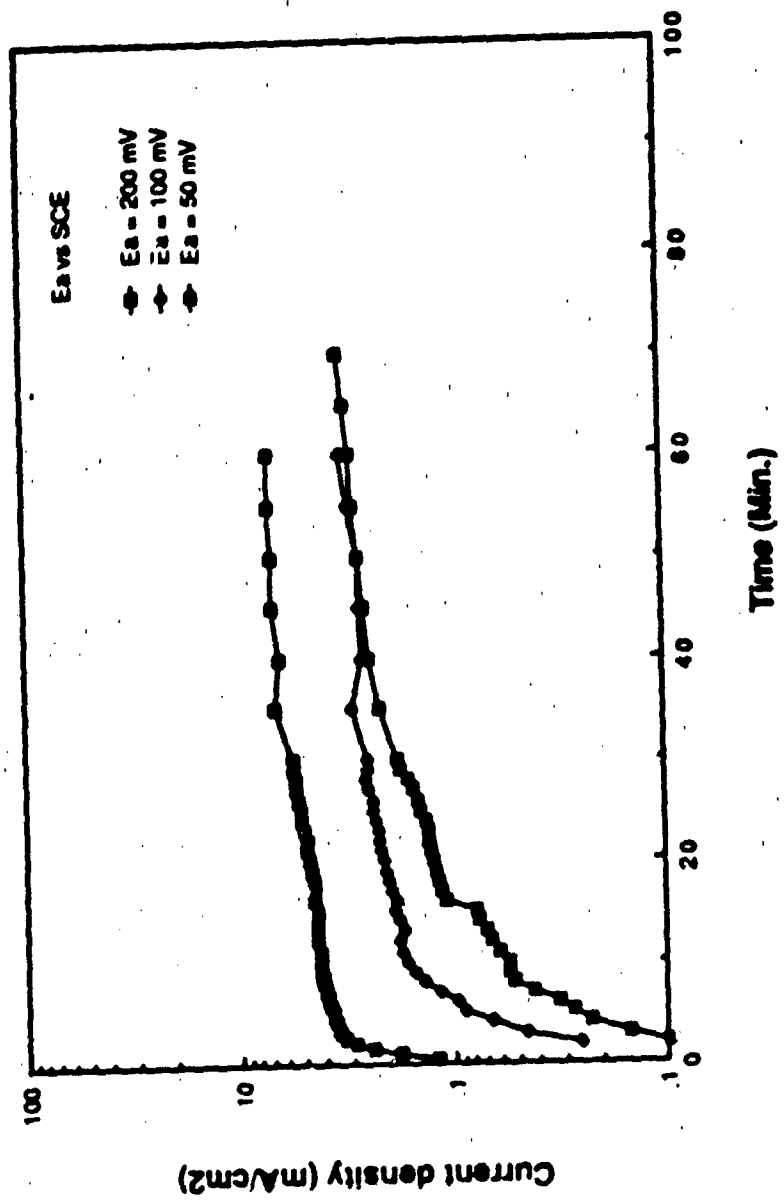


Figure 6. Current density vs time after scratching at constant potentials for 304L stainless steel in 0.5N NaCl solution (0 mg/L dissolved chlorine).

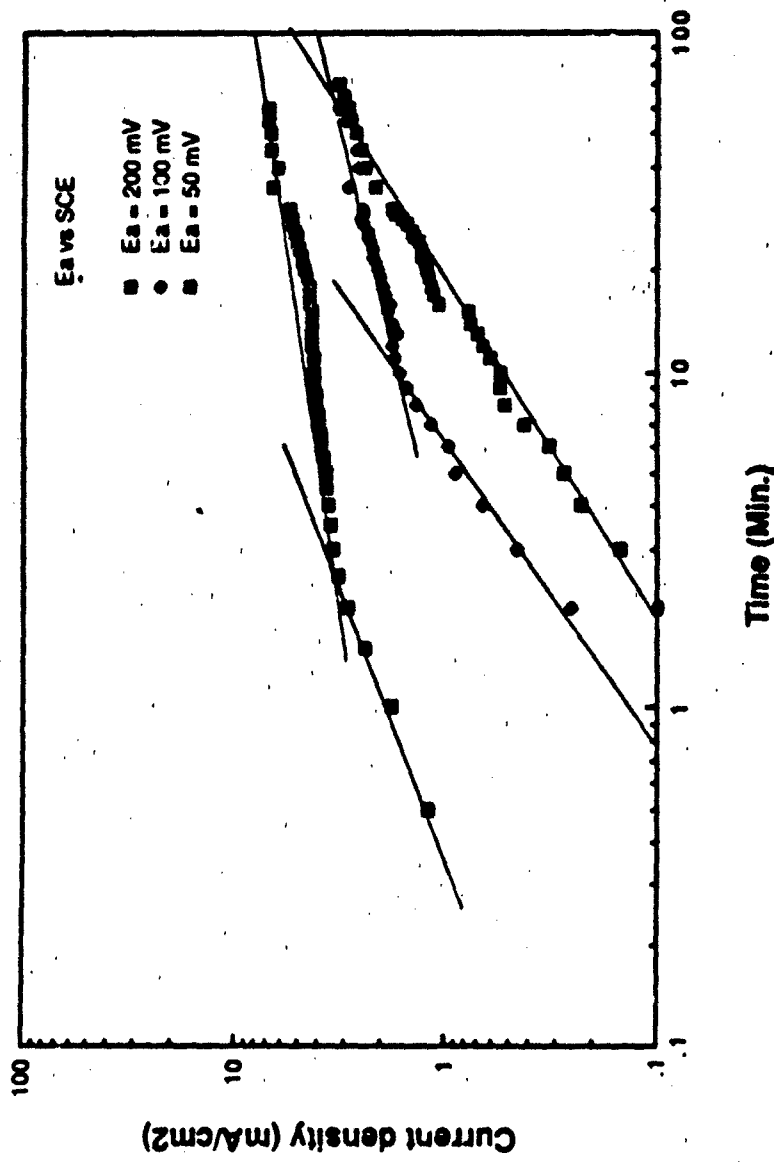


Figure 6. Current density vs time after scratching at constant potentials for 304L stainless steel in 0.5N NaCl solution (0 mg/L dissolved chlorine).

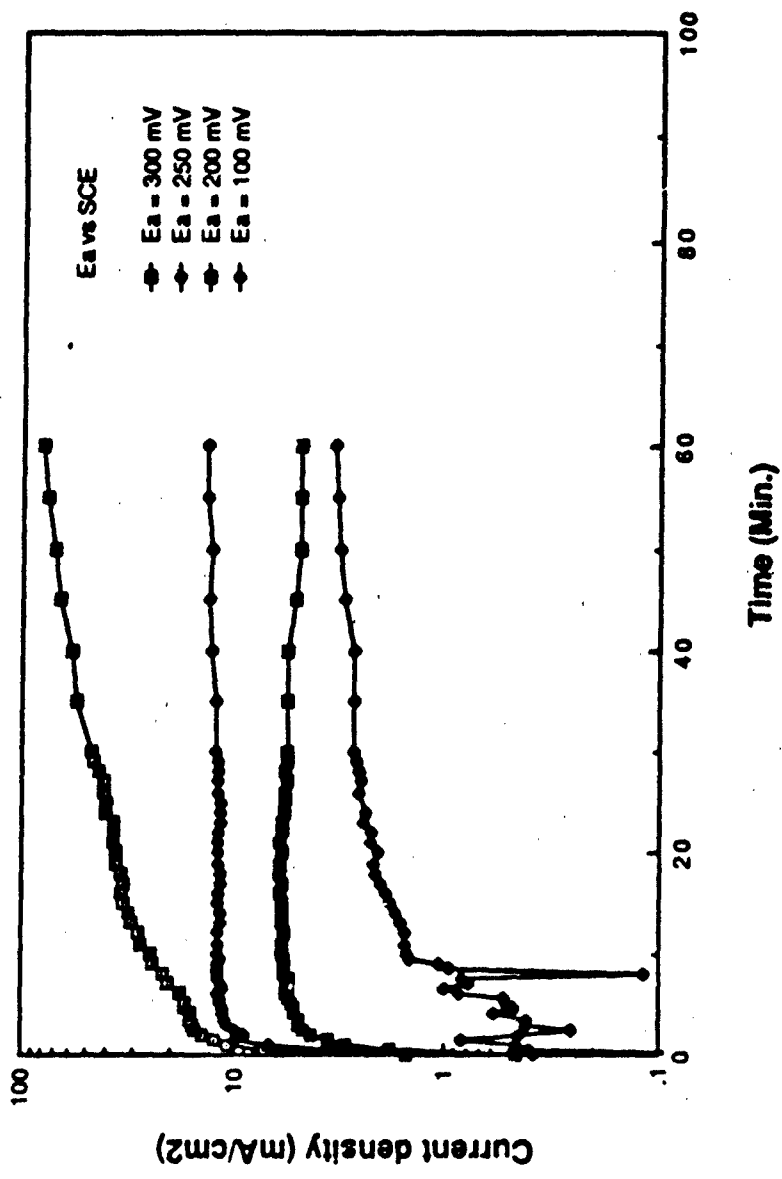


Figure 7. Current density vs time after scratching at constant potentials for 304L stainless steel in 0.5N NaCl solution with 20 mg/L dissolved chlorine.

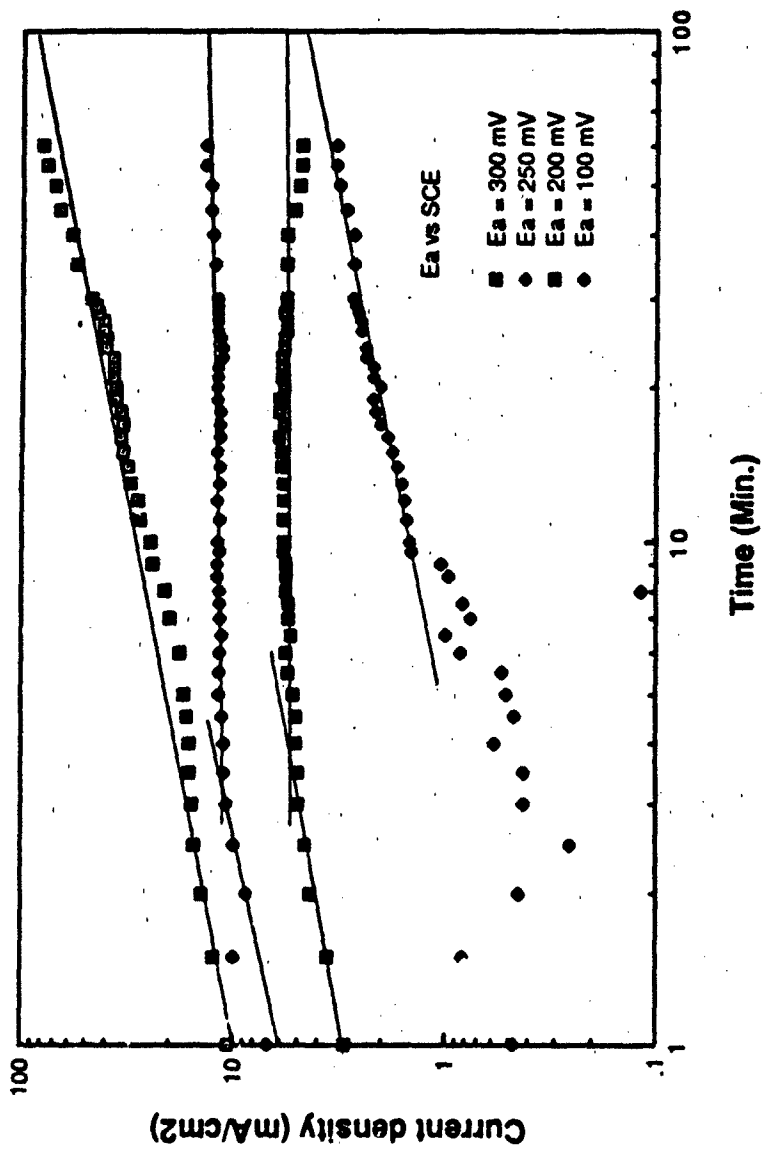


Figure 7. Current density vs time after scratching at constant potentials for 304L stainless steel in 0.5N NaCl solution with 20 mg/L dissolved chlorine.

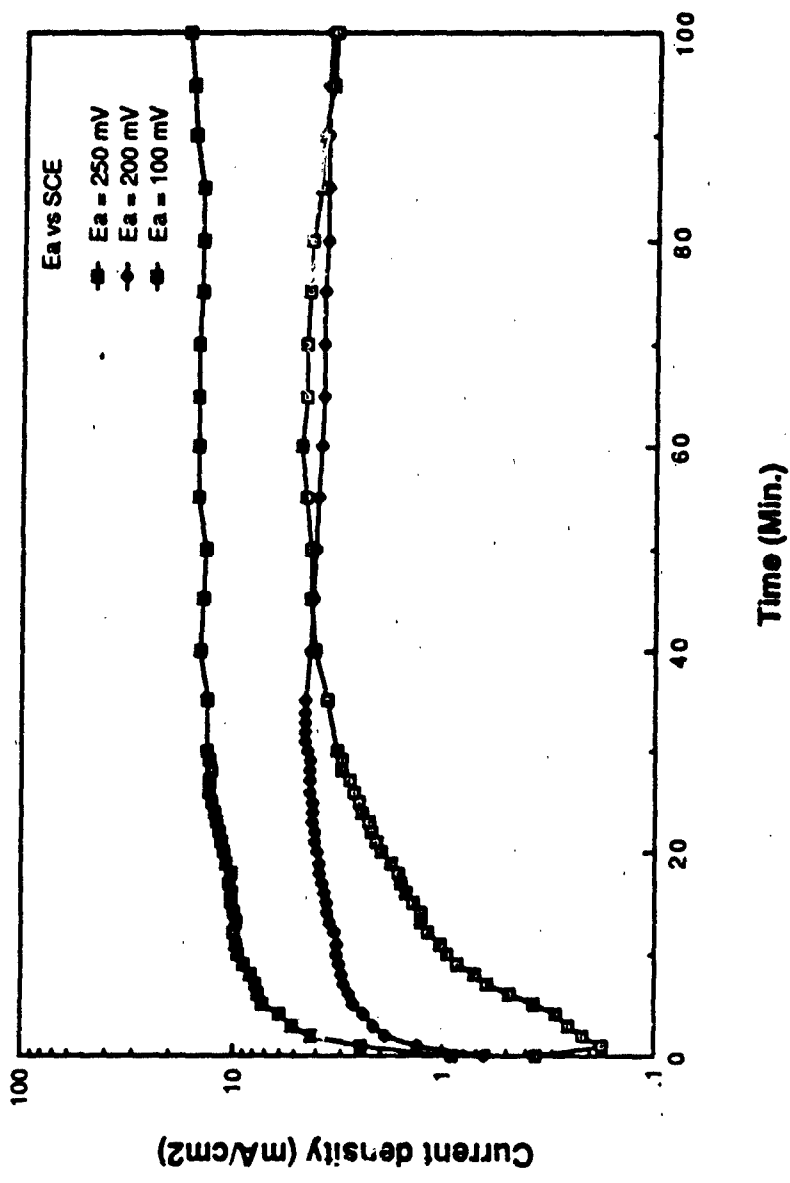


Figure 8. Current density vs time after scratching at constant potentials for 304L stainless steel in 0.5N NaCl solution with 60 mg/L dissolved chlorine.

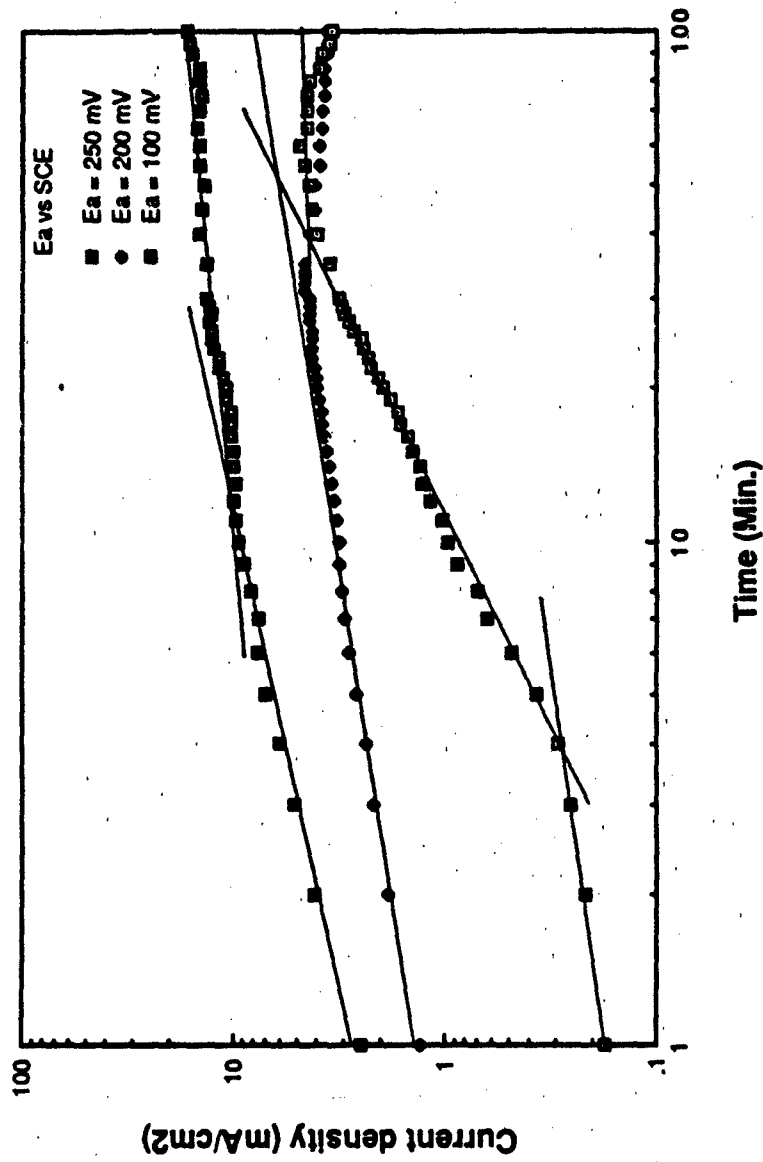


Figure 8. Current density vs time after scratching at constant potentials for 304L stainless steel in 0.5N NaCl solution with 60 mg/L dissolved chlorine.

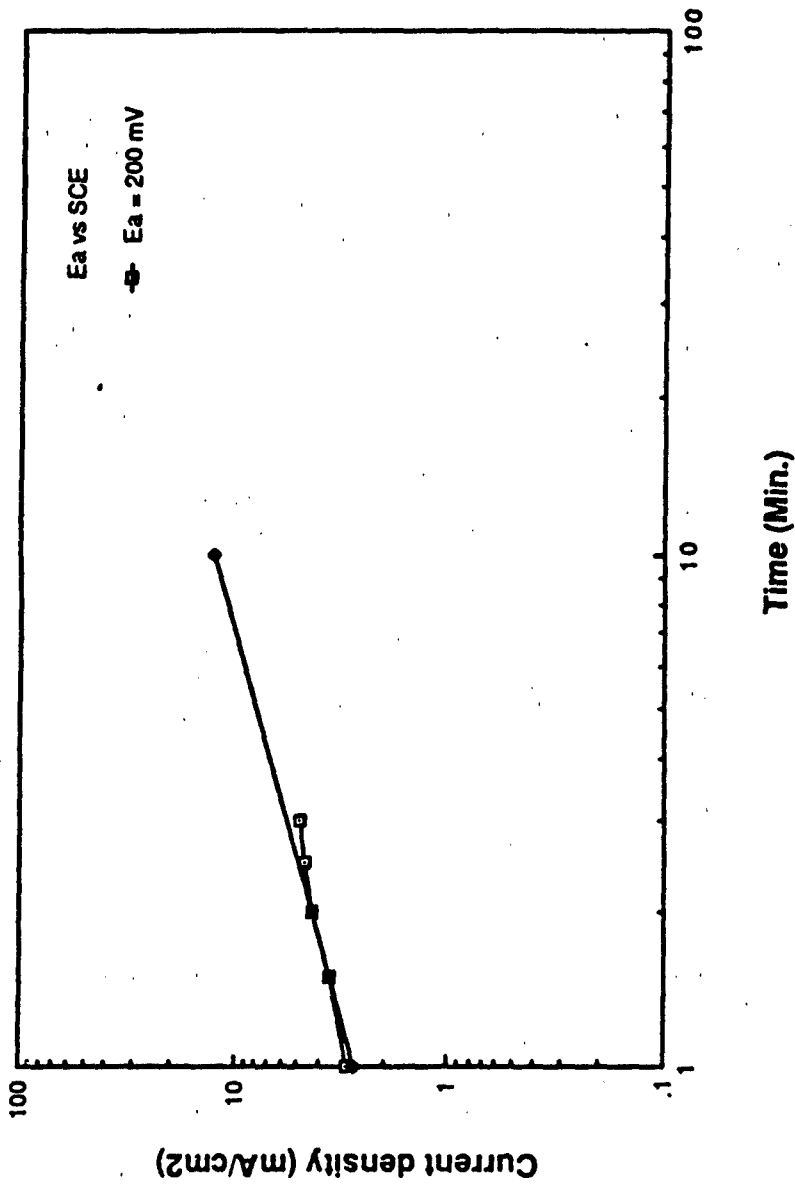


Figure 9 Correlation between measured slope of current density vs time with a hypothetical slope of 0.67 for transient period of localized corrosion of 304L stainless steel in 0.5N NaCl solution
(b) 20 mg/L dissolved chlorine.

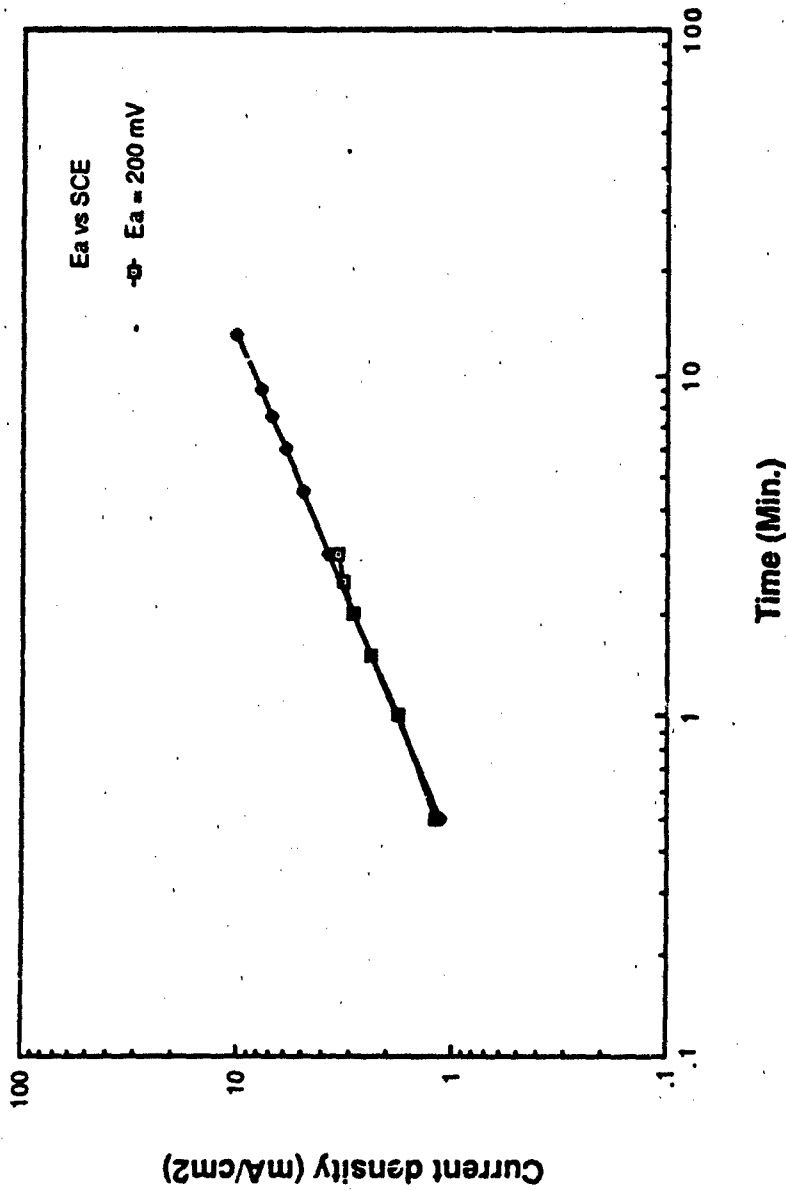


Figure 9 Correlation between measured slope of current density vs time with a hypothetical slope of 0.67 for transient period of localized corrosion of 304L stainless steel in 0.5N NaCl solution

(a) Unchlorinated



Fig. 10 Typical morphology of pits in 304L stainless steel in 0.5N NaCl solution. Pit morphology is unchanged by chlorination (a) optical cross section

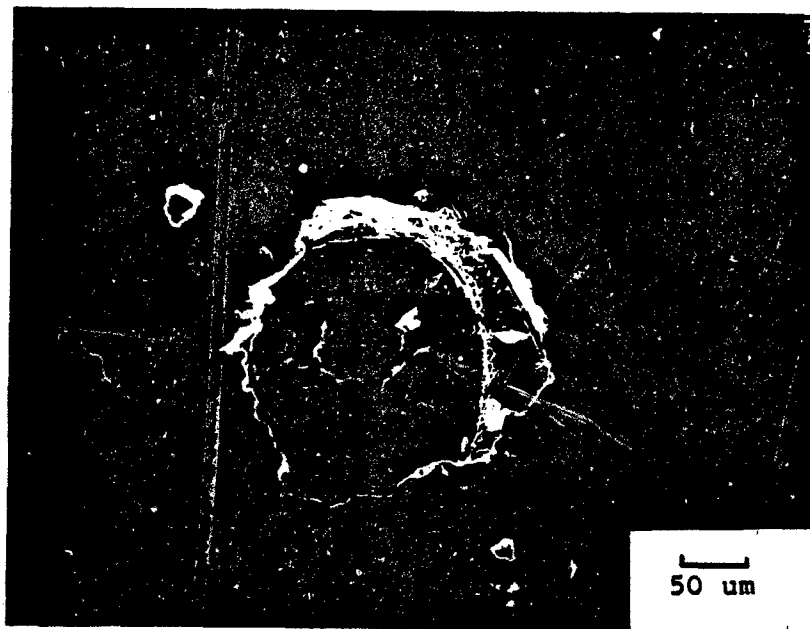


Fig. 10 Typical morphology of pits in 304L stainless steel in 0.5N NaCl solution. Pit morphology is unchanged by chlorination (b,c) scanning electron micrographs

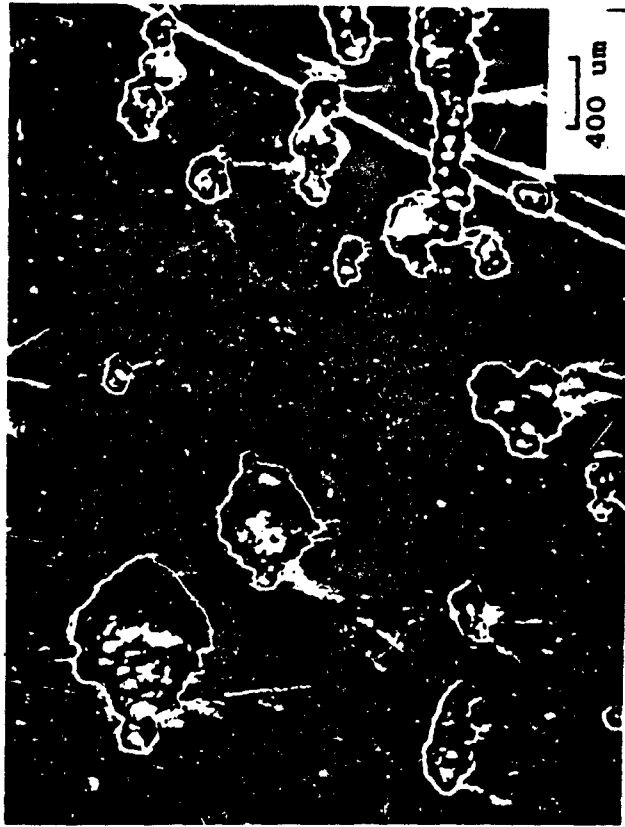


Figure 11 Pit distribution on 304L stainless steel in 0.5N NaCl solution with 20 mg/L dissolved chlorine.

Unrestricted

SECURITY CLASSIFICATION OF THIS PAGE

REPORT DOCUMENTATION PAGE

1a. REPORT SECURITY CLASSIFICATION Unrestricted		1b. RESTRICTIVE MARKINGS NONE	
2a. SECURITY CLASSIFICATION AUTHORITY		3. DISTRIBUTION/AVAILABILITY OF REPORT	
2b. DECLASSIFICATION/DOWNGRADING SCHEDULE			
4. PERFORMING ORGANIZATION REPORT NUMBER(S) 1		5. MONITORING ORGANIZATION REPORT NUMBER(S)	
6a. NAME OF PERFORMING ORGANIZATION Rensselaer Polytechnic Institute	6b. OFFICE SYMBOL <i>(If applicable)</i>	7a. NAME OF MONITORING ORGANIZATION	
6c. ADDRESS (City, State and ZIP Code) Troy, NY 12180-3590		7b. ADDRESS (City, State and ZIP Code)	
8a. NAME OF FUNDING/SPONSORING ORGANIZATION Office of Naval Research	8b. OFFICE SYMBOL <i>(If applicable)</i>	9. PROCUREMENT INSTRUMENT IDENTIFICATION NUMBER	
8c. ADDRESS (City, State and ZIP Code) 800 N. Quincy Street Arlington, VA 22217-5000		10. SOURCE OF FUNDING NOS.	
		PROGRAM ELEMENT NO.	PROJECT NO.
		TASK NO.	WORK UNIT NO.
11. TITLE (Include Security Classification) THE EFFECT OF DISSOLVED CHLORINE ON THE PITTING BEHAVIOR OF 304L STAINLESS STEEL IN A 0.5 N NaCl SOLUTION			
12. PERSONAL AUTHOR(S) H.H. Lu and D.J. Duquette			
13a. TYPE OF REPORT Technical	13b. TIME COVERED FROM 10/86 TO 10/89	14. DATE OF REPORT (Yr., Mo., Day) 89 10 15	15. PAGE COUNT 39
16. SUPPLEMENTARY NOTATION NONE			
17. COSATI CODES		18. SUBJECT TERMS (Continue on reverse if necessary and identify by block number)	
FIELD	GROUP	SUB. GR.	
		Corrosion, Stainless Steels, Dissolved Chlorine, Chloride Solutions	
19. ABSTRACT (Continue on reverse if necessary and identify by block number)			
<p>Electrochemical experiments were performed on a 304L stainless steel alloy in a 0.5 N NaCl solution as a function of chlorine content (0-180 mg/l). Experiments performed included a measurement of the corrosion potential as a function of time, the determination of the breakdown potential, and of the repassivation potential, utilizing cyclic polarization curves; and the use of a scratching electrode technique to measure the kinetic aspects of the breakdown of passivity. The addition of chlorine to a solution of pH5 in the concentration range of 20-60 ppm chlorine resulted in a significant shift in the corrosion potential in the noble direction. At higher concentrations of chlorine the corrosion potential shifts back toward that observed without chlorine additions. Chlorine also results in a monotonic shift in the breakdown potential, suggesting that the passive film is rendered more stable against the initiation of localized corrosion. However, the repassivation (see other side)</p>			
20. DISTRIBUTION/AVAILABILITY OF ABSTRACT UNCLASSIFIED/UNLIMITED <input checked="" type="checkbox"/> SAME AS RPT. <input type="checkbox"/> DTIC USERS <input type="checkbox"/>		21. ABSTRACT SECURITY CLASSIFICATION Unrestricted	
22a. NAME OF RESPONSIBLE INDIVIDUAL D.J. Duquette		22b. TELEPHONE NUMBER <i>(Include Area Code)</i> 518-276-6459	22c. OFFICE SYMBOL

potential exhibits a minimum in the chlorine concentration range where the corrosion potential exhibits a maximum. This data suggests that the rate of propagation of localized corrosion should be maximized in this chlorine regime (20-60 mg/l). When scratching electrode experiments are performed, the number of pits is minimized but the size of the pits is maximized. Analysis of the kinetic pit growth results suggest that, when the pits are small, the rate of pit growth is controlled by diffusion of corrosion products through the bulk aqueous phase, but, as the pits age, the mechanism changes, and pit growth is governed by diffusion through a solid or semi-solid film on the walls of the pits.